High Q Resonances in a Metallically Coated Wave-Chaotic Microcavity

Jia Qiu, Yajun Liu, Qin Wu, Kaijun Che, and Maowei Xie

***Abstract*—Optical resonances of a metallically coated wave-chaotic microcavity are investigated. Mode resonances with a low-contrast quality factor and distinct field patterns are demonstrated. Unlike the resonances in the dielectric chaotic-wave cavity where the refractive escape leads a high optical loss, the resonances in metallically coated cavity hold high quality factors with a low loss induced by metal dissipation. As a potential application, the metallically coated chaotic-wave microcavity could be used for a semiconductor laser source with dense modes lasing and accordingly a low spatial coherent emission.**

***Index Terms*—Chaotic-wave microcavity, surface plasmonic mode, low coherent light source.**

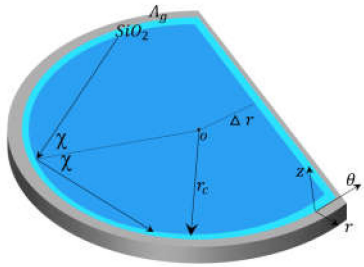

Fig. 1. Two dimensional schematic illustration of a wave-chaotic microcavity with D shape, which is laterally coated by silica (SiO_2) and silver (Ag) layers.

I. Introduction

SEMICONDUCTOR microcavity lasers with quasi-two-dimensional (2D) optical confinements have been extensively investigated in the past decades for on-chip generation of the high coherent signal source [1], [2]. One of representative 2D microcavities is whispering-gallery-mode (WGM) cavity, where WGMs are formed via the total and consecutive internal reflections of light wave on the cavity boundary and hold high quality (Q) factors $Q = \omega\tau$ and low mode volume V_m as ω and τ are resonance angular frequency and photon life time [3]. The strong enhancement of light-matter interaction with a figure of merit Q/V_m greatly reduces the pump gain, and ultra-low threshold microlasers have been widely developed [4]. Owing to that Q/V_m of WGMs confined in dielectric microcavity are distributed in a wide range, such as that fundamental WGMs hold much higher Q/V_m than that of radially higher-order WGM, added with a large free spectral rang, a fundamental WGM or a few radially low-order WGMs are excited for lasing in microcavity laser [5]. But for the applications, such as the optical generation of high speed physical random number [6], and full-field imaging and displays [7], a laser source with low time or spatial coherence is promising. Recently, dielectric asymmetric microcavities with fully chaotic ray dynamics (also called wave-chaotic cavity) have been used as resonant cavities for edge-emitting laser with low spatial coherence [8], where dense modes lasings in a spectral band are demonstrated as the resonant modes hold similar Q factors and distinct field patterns. In addition, Fabry-Pérot-like (FP-like) cavity with two carefully designed concave mirrors was further developed for a laser diode with low-time/spatial coherence [9], [10]. Thus, the edge-emitting semiconductor lasers with highly dense mode lasings and low time/spatial coherent emissions, have been achieved based on a dielectric wave-chaotic cavity or a FP-like cavity. Nevertheless, the refractive escape of the resonances in chaotic-wave cavity or FP-like cavity limits the mode Q factors to a low value. A relatively high pump threshold, which is inversely proportional to Q/V_m, is required.

Here, a metallically coated chaotic-wave cavity is proposed for high Q mode resonances. Unlike the resonances in dielectric cavity with a low Q factor due to the optical loss induced by the refractive escape, the resonances in the proposed metallically coated cavity hold a high Q factor with a low loss induced by metal dissipation. The metallically coated cavity, evanescently coupled with a wide waveguide on substrate for power output [11], are expected to find application of a compact laser source with low spatial coherence.

II. Wave Dynamics in a Metallically Coated WGM Cavity

The D shape microcavity is a well-studied system with chaotic-ray dynamics and here is considered as a wave-chaotic cavity. Part of circular cavity is removed along a straight cut and a D shape cavity is formed [12], [13]. A two dimensional (2D) schematic illustration of a metallically coated cavity is shown in Fig. 1. Here, a semiconductor microcavity, laterally coated by layers of silica (SiO_2) and silver(Ag), is considered [11], [14]–[16]. The SiO_2 layer usually functions as an insulator for the electrically pumped semiconductor devices, and could

Manuscript received March 31, 2022; revised May 11, 2022; accepted May 23, 2022. Date of publication May 30, 2022; date of current version June 8, 2022. This work was supported by the National Natural Science Foundation of China under Grant 61935018. *(Corresponding author: Kaijun Che.)*

The authors are with the School of Electronic Science and Engineering, Xiamen University, 361005 Fujian, China (e-mail: jiaqiu@stu.xmu.edu.cn; liuyajun@stu.xmu.edu.cn; wuqin@stu.xmu.edu.cn; chekaijun@xmu.edu.cn; xiemw@stu.xmu.edu.cn).

Digital Object Identifier 10.1109/JPHOT.2022.3178691

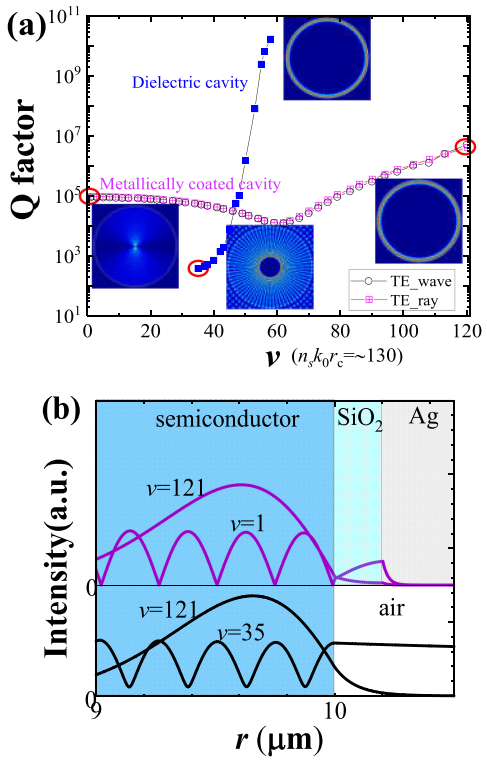

Fig. 2. (a) Q factors of TE WGMs in metallically coated cavity with v ranging from 0 to 121 as $n_s k_0 r_c = \sim 130$ obtained by both wave solutions (TE_wave) and ray tracing simulations (TE_ ray). Q factors of modes confined in dielectric cavity is added for comparison. Insets: the magnetic field patterns $|H_z|$ of modes with $v = 1$ and 121 in metallically coated cavity and with $v = 35$ and 121 in dielectric cavity, and (b) their field distributions along radial direction near cavity edge.

reduce optical loss induced by the metal dissipation as a buffer layer [17]–[19]. The radius of cavity is denoted as r_c and the normalized cutting width ε over r_c is given by $\varepsilon = 1 - \Delta r/r_c$.The electromagnetic fields in the cavity are described on cylindrical coordinate and the transverse electric (TE) modes with electric field in-plane (E_r, E_θ) are considered.

Here, for simplification, numerical investigations on 2D cavities are performed based on an effective refractive index [20]. We begin our analysis on resonances of a metallically coated WGM cavity. The mode Q factor is calculated by $Q = k_r/2k_i$ from the solution of the complex wave vector $k = k_r + ik_i$ based on the condition that tangential electric E_θ and magnetic fields H_z are continuous at the interfaces of the confinement layers [21]. The effective refractive indices of semiconductor (i.e., InGaAsP quantum wells wafer), SiO_2 and Ag here are set as $n_s = 3.2$, $n_{\mathrm{SiO2}} = 1.45$ and $n_{\mathrm{Ag}} = 0.14{+}11.35i$ in the 1550 nm band [22], respectively. If not stated otherwise, in the following, the thickness d_i of SiO_2 is fixed as 0.129λ as λ denotes the wavelength of light wave in vacuum (i.e., $d_i = 0.2$ μm for a $\lambda = 1.55$ μm). Fig. 2(a) shows Q factors of WGMs with the azimuthal number v ranging from 0 to 121 as $n_s k_0 r_c = \sim 130$, while k_0 is the wave vector in vacuum. It can be seen that the Q factor of WGM (denoted by TE_wave) has a minimum value as $v = 61$ and there are many modes with Q factor difference less than one-order of magnitude. For comparison, we also calculate the mode Q factor from the light ray propagation in the cavity (denoted by TE_ray). By comparing the angular momentum or wave vector in θ direction in ray picture (described as $n_s k_0 \sin\chi$) with that in wave picture (described as $v/\ r_c$) [23], the sin χ of WGM with a v is obtained as

$$\sin\chi = \frac{v}{n_s k_0 r_c} \tag{1}$$

of which χ is the incident angle of light ray on the cavity boundary (as shown in Fig. 1). And the Q factor of corresponding mode is calculated by

$$Q = -\frac{2n_s k_0 r_c \cos\chi}{\ln R} \tag{2}$$

where R is the reflectivity of incident light on SiO_2 and Ag layers. The results shown in Fig. 2(a) indicate that the Q factor obtained from the ray picture is consistent with the Q factor obtained from the wave solution. For comparison, the modes in dielectric cavity with the same size are also considered and the Q factors are given in Fig. 2(a) with v ranging from 35 to 58. Owing to the over small Q factors for modes with v less than 35(whose incident angle is less than the critical angle) and the ultra-high Q factors for modes with v greater than 58 (whose incident angle is greater than the critical angle), the Q factors of these modes are thus not given. It can be found that the Q factors of modes in dielectric cavity vary from $\sim 10^2$ ($v = 35$) to $\sim 10^{10}$ ($v = 58$) and show a much larger contrast than that of modes confined metallically coated cavity. The highest-order mode with $v = 1$ in the metallically coated cavity still holds a Q factor of $\sim 8\times 10^4$ while the mode in dielectric cavity with $v = 35$ holds a low Q factor of only $\sim 10^2$ due to the refractive escape of light wave. The magnetic field patterns $|H_z|$ of modes with $v = 1$ and 121 in metallically coated cavity and modes with $v = 35$ and 121 in dielectric cavity are displayed by the insets of Fig. 2(a) and the field distributions along radial direction near cavity edge are plotted in Fig. 2(b). The low field intensity in metal is observed, which allows low optical dissipation and accordingly high Q factor resonances [15], [16]. In circular cavity, the WGMs feature regular field patterns and hold a large contrast Q factor, the lasing with a single mode or a dominant mode is usually observed. If the contrast of mode Q factor further decreases so that the modes have similar Q factors, and additionally they hold distinct field patterns, as presented in [8], the gain saturation among the lasing modes in active cavity could be suppressed and multimode lasings are expected. In the following, the resonances in a metallically coated microcavity with D shape are investigated.

III. Resonances in a Metallically Coated Microcavity With D Shape

To investigate the resonances evolution in the metallically coated D shape cavity with ε in a range of 0 and 1, we resort to a full–vectorial eigenmode solver based on the finite element method (FEM) [24]. Fig. 3(a) displays the resonant spectra with 60 modes at $n_s k_0 r_c = \sim 130$ as $\varepsilon = 0.0, 0.7$ and 1, corresponding to a cavity with radius of $r_c = 10$ μm for the wave with $\lambda = 1.55$ μm. For the WGM cavity ($\varepsilon = 0$), the Q factor ranges from 10^4 to 5×10^6, exhibiting a high contrast, while that of

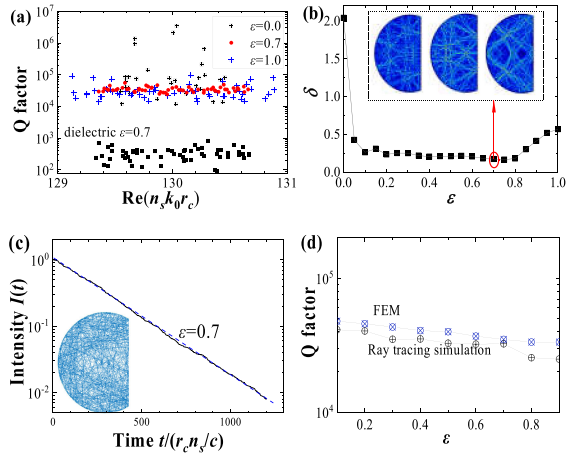

Fig. 3. (a) Spectra of TE modes in a metallically coated D shape cavity with $\varepsilon = 0$, 0.7 and 1 and in a dielectric D shape cavity with $\varepsilon = 0.7$. (b) The Q factor contrast δ of the considered 60 modes versus ε ranging from 0 to 1. The insets show the field patterns of three modes with nearly the same Q factor as $\varepsilon = 0.7$ (c) The intensity decay of chaotic ray (mode) based on the ray tracing simulations, the inset shows a chaotic ray trajectory of 500 reflections on the cavity boundary. (d) The Q factor of the chaotic rays(modes) based on the ray tracing simulations and the mean mode factors $\langle Q \rangle$ based on wave simulations with a ε ranging from 0.1 to 0.9. All the waves are considered with $n_s k_0 r_c = \sim 130$.

modes in a cavity with $\varepsilon = 0.7$ ranges from 2.2×10^4 to 5.6×10^4, showing a much lower contrast. From the view of symmetry, the Q factors of modes confined in the semicircular cavity ($\varepsilon = 1$) present relatively high-contrast as well. For comparison, the resonant spectra of a dielectric D shape cavity with $\varepsilon = 0.7$ is also presented. It can be found that the mode Q factors are less than that of modes in metallically coated cavity by nearly 2 orders. A factor $\delta = \sigma/\langle Q \rangle$ is used to describe Q factor contrast: the ratio of the standard deviation σ of Q factor to the mean value $\langle Q \rangle$ of the considered modes covering a spectrum band of $\sim$2 of $n_s k_0 r_c$. Fig. 3(b) plots δ for different cutting width ε. It shows that a slight modification on cavity geometry ($\varepsilon = 0.1$ for instance) leads a small δ ($\sim$0.4) and there is a minimum value of $\delta \sim 0.17$ near $\varepsilon = 0.7$, at which the insets present the distinct field patterns of three modes with nearly the same Q factor. In addition, 135 modes covering a spectrum band of 2 around $n_s k_0 r_c = 195$ are also considered in a larger cavity with $r_c = 15$ μm, we find that δ has nearly the same relationship with ε. Thus, a minimum value of δ can be obtained as $\varepsilon = 0.7$ in a cavity with an $n_s k_0 r_c$ far greater than 10^2. We also compare $\langle Q \rangle$ with the Q factor of mode with chaotic ray trajectory in a D shape cavity as $n_s k_0 r_c = \sim 130$. The evolution of ray intensity $I(t)$ with a chaotic trajectory (500 times reflections are presented by inset) is shown in Fig. 3(c) as the propagating time t (normalized over $r_c n_s/c$, c is the light speed in vacuum) beyond 10^3 in a cavity with ε= 0.7. The ray tracing simulations indicate that $I(t)$ decays exponentially ($I(t) \sim e^{-t/\tau}$) and the Q factor is estimated from power decaying time τ. As presented in Fig. 3(d), the Q factor of a mode with a chaotic ray trajectory decreases monotonously as ε increases from 0.1 to 0.9 (integrable cavities with $\varepsilon = 1$ and 0 are not considered here), and $\langle Q \rangle$ of modes based on FEM simulations versus ε is also given for comparison. The results indicate that the Q factor of

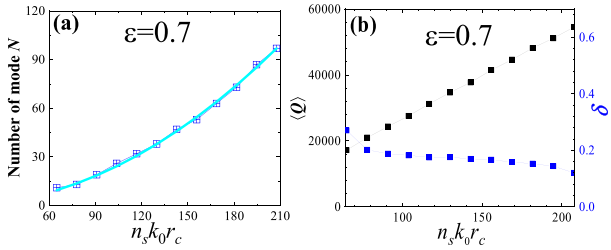

Fig. 4. (a) Number of resonances, (b) mean Q factor $\langle Q \rangle$, and Q factor contrast δ versus $n_s k_0 r_c$ as $\varepsilon = 0.7$.

mode with a chaotic ray trajectory is consistent with $\langle Q \rangle$. Thus, as cavity size, such as the radius of cavity r_c, is further increased, $\langle Q \rangle$ can be predicted from the ray tracing simulation since that it is quite computationally expensive for wave simulations on a cavity with a $n_s k_0 r_c$ beyond 10^3.

The number of modes N in a spectra band in a chaotic-wave cavity, associated with the number of lasing modes [8], is one of the important parameters taking effect on the spatial coherence of a semiconductor microlaser, especially for a cavity with $n_s k_0 r_c$ far greater than the wavelength of resonant wave. In Fig. 4(a), the number N of modes covering a spectrum band of 10 nm at $\lambda = 1.55$ μm versus $n_s k_0 r_c$ ranging from $\sim$64 to $\sim$208 is shown. The fitted solid line presents $0.175 S_d$ as S_d denotes the surface area of D shape cavity and is calculated by $S_d = r_c^2(\pi - \cos^{-1}(1-\varepsilon) + (1-\varepsilon)\sqrt{\varepsilon(2-\varepsilon)})$. Thus, we can simply find N from S_d. Take a cavity with $n_s k_0 r_c = 1297$ ($r_c = \sim 100$ μm) and $\varepsilon = 0.7$ as an example, N is estimated to be 3783. In addition, the relations between $\langle Q \rangle$, δ and $n_s k_0 r_c$ are also studied and the results are displayed in Fig. 4(b). It shows $\langle Q \rangle$ is highly linear to $n_s k_0 r_c$ and the relationship is extracted as $\langle Q \rangle = 566 + 261 n_s k_0 r_c$ and $\langle Q \rangle$ is estimated to be 3.39×10^5 when $n_s k_0 r_c$ equals 1297. Moreover, as presented, δ decreases from 0.27 to 0.12 as $n_s k_0 r_c$ increases from 64 to 208 and will tend to 0 if $n_s k_0 r_c$ further increases. For the D shape cavity with different arc circumferences, such as cavity with $\varepsilon = 0.3$ or 0.9, N has the same relationship with S_d, but the $\langle Q \rangle$ will not be simply linear with $n_s k_0 r_c$ due to the large δ.

It is should be emphasized that there is no edge emission for the microlaser with a metallically coated cavity. Two ways are proposed for emission collection. One is collecting the lasing emission directly from the substrate of semiconductor chip [25]. Another is to introduce a waveguide on the substrate for the directional emission coupling via evanescently wave [11]. Both power coupling routes inevitably degrade the resonances. Thus, the total Q factor of resonances Q_{total} is not only associated with the optical loss induced by the metal dissipation ($Q_{dissipation}$), buth also associated with the power collection $Q_{coupling}$ ($1/Q_{total} = 1/Q_{dissipation} + 1/Q_{coupling}$). A trade-off between the laser threshold determined by Q_{total} and the output lasing power determined by $Q_{coupling}$ should be considered while designing a coupling waveguide, such as the gap between the active layer and the waveguide, and the waveguide width and height etc.

IV. Conclusion

In conclusion, we have performed the theoretical investigations on the resonance characteristics of a metallically coated wave-chaotic microcavity. For a D shape cavity with a cutting width, a low-contrast (0.17 for resonances with $n_s k_0 r_c = \sim 130$) and high Q resonances with distinct field patterns is demonstrated. The number of modes in a spectral band and the mean Q factor are linearly proportional to the surface area of cavity and $n_s k_0 r_c$, respectively. The semiconductor lasers, with resonances of a metallically coated wave-chaotic microcavity, are expected for the applications of compact light sources with dense mode lasing and accordingly a low spatial-coherence.

References

[1] K. J. Vahala, "Optical microcavities," *Nature*, vol. 424, pp. 839–846, Aug. 2003.

[2] H. Cao and J. Wiersig, "Dielectric microcavities: Model systems for wave chaos and non-Hermitian physics," *Rev. Modern Phys.*, vol. 87, no. 1, pp. 61–111, Jan. 2015.

[3] J. Ward and O. Benson, "WGM microresonators: Sensing, lasing and fundamental optics with microspheres," *Laser Photon. Rev.*, vol. 5, no. 4, pp. 553–570, Jul. 2011.

[4] L. He, S. K. Ozdemir, and L. Yang, "Whispering gallery microcavity lasers," *Laser Photon. Rev.*, vol. 7, no. 1, pp. 60–82, Jan. 2013.

[5] Q. Song, H. Cao, S. T. Ho, and G. S. Solomon, "Near-IR subwavelength microdisk lasers," *Appl. Phys. Lett.*, vol. 94, no. 6, Feb. 2009, Art. no. 061109.

[6] A. Uchida *et al.*, "Fast physical random bit generation with chaotic semiconductor lasers," *Nature Photon.*, vol. 2, pp. 728–732, Dec. 2008.

[7] M. Nixon, B. Redding, A. A. Friesem, H. Cao, and N. Davidson, "Efficient method for controlling the spatial coherence of a laser," *Opt. Lett.*, vol. 38, no. 19, pp. 3858–3861, Oct. 2013.

[8] B. Redding *et al.*, "Low spatial coherence electrically pumped semiconductor laser for speckle-free full-field imaging," *Proc. Nat. Acad. Sci.*, vol. 112, no. 5, pp. 1304–1309, Feb. 2015.

[9] K. Kim, S. Bittner, Y. Zeng, S. F. Liew, Q. J. Wang, and H. Cao, "Electrically pumped semiconductor laser with low spatial coherence and directional emission," *Appl. Phys. Lett.*, vol. 115, no. 7, Aug. 2019, Art. no. 071101.

[10] K. Kim *et al.*, "Massively parallel ultrafast random bit generation with a chip-scale laser," *Science*, vol. 371, no. 6532, pp. 948–952, Feb. 2021.

[11] V. D. Calzadilla *et al.*, "Waveguide-coupled nanopillar metal-cavity light-emitting diodes on silicon," *Nature Commun.*, vol. 8, no. 1, Feb. 2017, Art. no. 14323.

[12] Q. F. Yao *et al.*, "High-Q modes in defected microcircular resonator confined by metal layer for unidirectional emission," *Opt. Exp.*, vol. 21, no. 2, pp. 2165–2170, Jan. 2013.

[13] S. Ree and L. E. Reichl, "Classical and quantum chaos in a circular billiard with a straight cut," *Phys. Rev. E*, vol. 60, no. 2, pp. 1607–1615, Aug. 1999.

[14] K. J. Che, Y. D. Yang, and Y. Z. Huang, "Multimode resonances in metallically confined square-resonator microlasers," *Appl. Phys. Lett.*, vol. 96, no. 5, Feb. 2010, Art. no. 051104.

[15] Y. F. Xiao *et al.*, "High-Q exterior whispering-gallery modes in a metal-coated microresonator," *Phys. Rev. Lett.*, vol. 105, no. 1, Oct. 2010, Art. no. 153902.

[16] B. Min *et al.*, "High-Q surface-plasmon-polariton whispering-gallery microcavity," *Nature*, vol. 457, pp. 455–459, Jan. 2009.

[17] R. F. Oulton, V. J. Sorger, D. A. Genov, D. F. P. Pile, and X. Zhang, "A hybrid plasmonic waveguide for subwavelength confinement and long-range propagation," *Nature Photon.*, vol. 2, no. 8, pp. 496–500, Aug. 2008.

[18] K. J. Che, Y. D. Yang, and Y. Z. Huang, "Mode characteristics for square resonators with a metal confinement layer," *IEEE J. Quantum Electron.*, vol. 46, no. 3, pp. 414–420, Mar. 2010.

[19] M. P. Nezhad *et al.*, "Room-temperature subwavelength metallo-dielectric lasers," *Nature Photon.*, vol. 4, pp. 395–399, Aug. 2010.

[20] M. E. Chin, D. Y. Chu, and S. T. Ho, "Estimation of the spontaneous emission factor for microdisk lasers via the approximation of whispering gallery modes," *J. Appl. Phys.*, vol. 75, no. 7, pp. 3302–3307, Apr. 1994.

[21] K. J. Che, C. X. Chu, C. L. Guo, D. Zhang, and Z. P. Cai, "Polarization dependent mode dynamics of metallic hybrid laser micro-resonator," *Opt. Commun.*, vol. 338, pp. 128–132, Oct. 2015.

[22] E. D. Palik, *Handbook of Optical Constants of Solids*, vol. 3, San Diego, CA, USA: Academic Press, 1998.

[23] M. Hentschel and H. Schomerus, "Fresnel laws at curved dielectric interfaces of microresonators," *Phys. Rev. E*, vol. 65, Apr. 2002, Art. no. 045603.

[24] M. Oxborrow, "Traceable 2-D finite-element simulation of the whispering-gallery modes of axisymmetric electromagnetic resonators," *IEEE Trans. Microw. Theory Techn.*, vol. 55, no. 6 pp. 1209–1218, Jun. 2007.

[25] M. T. Hill *et al.*, "Lasing in metallic-coated nanocavities," *Nature Photon.*, vol. 1, no. 10, pp. 589–594, Sep. 2007.